

HU9013652

KFKI-1989-47/A

P. LÉVAI
B. LUKÁCS
J. ZIMÁNYI

**ENTROPY CONTENT FROM
STRANGE PARTICLE RATIOS
IN THE E802 EXPERIMENT**

**Hungarian Academy of Sciences
CENTRAL
RESEARCH
INSTITUTE FOR
PHYSICS**

BUDAPEST

KFKI-1989-47/A
PREPRINT

**ENTROPY CONTENT
FROM STRANGE PARTICLE RATIOS
IN THE E802 EXPERIMENT**

P. LÉVAI, B. LUKÁCS, J. ZIMÁNYI

**Central Research Institute for Physics
H-1526 Budapest 114, P.O.B. 49, Hungary**

P. Léval, B. Lukács, J. Zimányi: Entropy content from strange particle ratios in the E802 experiment.
KFKI-1989-47/A

ABSTRACT

A method is given to reconstruct the local state of a heavy ion collision which produced the detected particles. Only some particle ratios are needed; in the simplest case 2 of them determines the local state if it was in complete thermodynamic equilibrium, and further ones check this last assumption. Applying the method on the available data of the E802 experiment, $T \approx 120$ MeV, $n/n_0 \approx 0.4$ and $S/N_B \approx 14$ is obtained, which is a reasonable break-up stage.

П. Левай, Б. Лукач, И. Зимани: Энтропия, определенная на основе отношений редких частиц, в эксперименте E802. KFKI-1989-47/A

Аннотация

Дается метод для определения локальных термодинамических данных состояния столкновения тяжелых ионов, испускающего детектированные частицы. Требуются лишь несколько отношений, в простых случаях 2 из них определяют локальное состояние, если оно было в полном термодинамическом равновесии, а остальные отношения применяются для проверки этого предположения. Прилагая этот метод к эксперименту E802, получается, что: $T \approx 120$ МэВ, $n/n_0 \approx 0.4$, $S/N_B \approx 14$, что кажется разумным конечным состоянием.

Léval P., Lukács B., Zimányi J.: Az E802 kísérleti entrópiája ritka részecske arányokból meghatározva. KFKI-1989-47/A

KIVONAT

Módszerrel adunk a detektált részecskéket kibocsátó lokális állapot rekonstruálására nehéziontúkörzésekben. Csak néhány részecskearányt kell használni; a legegyszerűbb esetben kettő meghatározza a lokális állapotot, ha az teljes termodinamikai egyensúlyban volt, és a tövábbiak ellenőrzik e feltevést. A módszert az E802 kísérlet hozzáférhető adataira alkalmazva adódik: $T \approx 120$ MeV, $n/n_0 \approx 0.4$ és $S/N_B \approx 14$, ami ésszerű feltörési állapotnak tűnik.

1. INTRODUCTION

Heavy ion reactions enable us to reach very hot and/or dense states of matter worthy for study but hopeless to form in any other way. However, the wanted states are transient, so one has to reconstruct their data from the detected fragments of the detonation, belonging to a cool dilute and expanding final state. This fact results in two disjoint limitations when looking for the characteristics. First, the reconstruction is more or less model dependent. (E.g. one has to make assumptions about interactions, freeze out, etc.) This problem may be technically serious, however is very familiar, and, anyways, one performs such experiments just for finding out the interactions. But, second, generally the reconstruction is not even direct.

Consider e.g. the temperature. One could measure temperature by observing the slope of the energy distribution of detected particles. However, this gives an *apparent* temperature, composed from true local temperature and average kinetic energy of expansion [1][2][3]. The same is true for energy density as well. In addition, above cca. 2 GeV/nucleon beam energy even an estimation based on the initial kinetic energies becomes ill-founded due to incomplete stopping [4], when the beam energy converts only partially into heat and compression. Clearly, the only *local* thermodynamic data which are identical in the matter (after hadrochemical transmutations have been completed) and at the detector are the particle ratios

$$R_k^i = N^i / N^k = n^i / n^k \quad (1.1)$$

Interestingly enough, in some cases these ratios are sufficient to locate the observed state in the thermodynamic state space. In this paper we discuss the possibility of such a reconstruction, show an explicit example for it, and by this way try to determine some properties of the state produced in the E802 experiment.

2. THE THERMODYNAMIC STATE SPACE

Consider a thermodynamical system with the independent extensives: volume V , energy E and particle number N^i . Then the local state is characterized by the densities e and n^i . The appropriate potential is [5] the entropy S , but now the density $s=S/V$ is sufficient,

$$s = s(e, n^i) \quad (2.1)$$

and the entropic intensives come as

$$\begin{aligned} \frac{1}{T} &= \frac{\partial s}{\partial e} \\ -\frac{\mu_i}{T} &= \frac{\partial s}{\partial n^i} \\ \frac{p}{T} &= s - \frac{1}{T}e - \sum \frac{\mu_i}{T}n^i \end{aligned} \quad (2.2)$$

Therefore any thermodynamic quantity can be calculated if the form of the potential $s(e, n^i)$ and the specific values of parameters e, n^i are known. The form of the potential belongs to the specific model and will not be discussed here. Our question is, how to deduce the complete set of extensive densities (or any complete set of local thermodynamic variables) from observables provided the potential function is of a known form.

By complete Legendre transformation one can substitute all extensive densities by intensives. Then p/T is the potential:

$$\frac{p}{T} = \frac{p}{T} \left(\frac{1}{T}, -\frac{\mu_i}{T} \right) \quad (2.3)$$

In our equilibrium situation then the independent quantities are $1/T, -\mu_i/T$ and $-\mu_e/T$. By partial Legendre transformation we have a set of variables containing some extensive densities and the intensives conjugate to the other ones.

Now, consider a mixture of particle components $i = 1 \dots \nu$, in complete chemical equilibrium. Then there is a number of algebraic relations amongst the chemical potentials, consequently the number of independently measurable ratios R_i^i i.e. $\nu - 1$ may be not less than the number of independent local thermodynamic data ((number of independent μ 's) + 1).

As a physical example (which is just the topic of this paper), consider a mixture of $\nu > 3$ hadronic components (nucleons, mesons, hyperons etc.) in complete chemical

equilibrium. In such a state the number of *independent* particle degrees of freedom is 2, according to the only conserved charges N^B (total baryon charge) and N^S (total strangeness). Moreover, if this state has been produced in a heavy ion collision, then, from the initial state,

$$N^S \equiv 0$$

Therefore then the complete set of independent extensive densities is

$$\{\epsilon, n^B\}$$

i.e. 2 data. So we can determine the local state from 2 measured particle ratios; further ones can check the assumptions.

In most cases the number of independent measurable particle ratios is > 2 . Thus one could express first two preselected ratios R_1, R_2 as functions of the extensive densities remaining independent after imposing chemical equilibrium, i.e. of ϵ, n^B, n^S . Then $n^S \equiv 0$, so

$$R_\alpha = R_\alpha(\epsilon, n^B); \quad \alpha = 1, 2$$

By inverting these equations one arrives at

$$\epsilon = \epsilon(R_\alpha) \tag{2.3a}$$

$$n^B = n^B(R_\alpha) \tag{2.3b}$$

and then every local quantity can be written as a function of R_α .

Nevertheless, this transformation of the thermodynamic parameters is *not* a Legendre transform. Consequently, by performing it we leave the framework of the canonical structure of thermodynamics. (The new variables are neither extensive densities, nor intensives.) So one has to see if no loss of information happens.

Here one may make use of the fact that there is a Riemannian geometry in the thermodynamic state space [6][7][8]. In a Riemannian space one may use *any* set of independent coordinates and may perform arbitrary regular coordinate transformations. So, we only have to investigate the completeness of thermodynamic information in connection with this Riemannian structure.

Using extensive densities as coordinates x^i , the metric tensor of the state space, measuring the fluctuations, can be obtained as

$$g_{ik} = - \frac{\partial^2 s}{\partial x^i \partial x^k} \tag{2.4}$$

Integrating back twice, from this g_{ik} any information, measurable purely by thermodynamic means, can be obtained, including the entropy function, up to zero point

constants of intensives [9][10] (which cannot be measured in thermodynamics, but need Third Law type prescriptions to be fixed). Thus g_{ik} carries all the relevant thermodynamic information.

Introducing an arbitrary new set of coordinates

$$x^{i'} = x^i(x^k) \quad (2.5)$$

the metric tensor transforms as [7], [11]

$$g'_{ik} = g_{rs} \frac{\partial x^r}{\partial x^{i'}} \frac{\partial x^s}{\partial x^{k'}} \quad (2.6)$$

Now, from the new g'_{ik} and from the functions $x^{i'}(x^k)$ the metric tensor g_{ik} in the canonical coordinates x^i can be reconstructed, and thence the entropy function. Therefore any nondegenerate coordinate transformation (2.5) keeps the complete thermodynamic information. (Of course, generally in the new coordinates not the entropy function contains the full information.)

Hence one could jump to the conclusion that then R_a span the thermodynamic state space as well as the independent densities ϵ, n^B do, and therefore by measuring two particle ratios one could locate the state uniquely in the state space. However, this is true only locally, not globally.

Consider eqs. (2.3a),(2.3b) as coordinate transformations of type (2.5). Such transformations are regular if the Jacobian does not vanish, which is assumed here and can be checked for a given model system. However, this regularity does not yet guarantee that the transformation be invertible; i.e. it is possible that two different sets of the extensive densities will coincide after the transformation. The condition that this do not happen is roughly that the new variables must be monotonous functions of the old ones. This is generally not true, specially for particle ratios. In this case a value pair R_1, R_2 will belong to more than one thermodynamic state, however separated by a nonzero distance in the state space. Then, measuring a third ratio R_3 , too (necessary anyways for checking the equilibrium assumption), the actual value of the third ratio will select the appropriate "Riemannian sheet" where the actual state is located.

3. ENTROPY IN HEAVY ION COLLISIONS

The entropy production in a collision is maximal if the stopping is complete. The corresponding S/N specific entropy value can be estimated in a one-fluid dynamical model or by shock-wave approximation; the specific value is of course model-dependent, but at 14.5 GeV/nucleon beam energy one can get cca. 9.5 unit for hadronic matter and cca. 11 unit for quark plasma. One fluid calculations show that the dominant part of entropy is produced *until* maximal compression [12],[13] (some 90 % of the final value). The reason is simple to understand in phenomenologic language: the velocity field is much smoother in the expansion stage, therefore viscous effects are weaker. This is partly true even with transparency, therefore we may assume still that the observed S/N is more or less characteristic for maximal compression.

The final state just before breakup is a dilute gas. Therefore then S/N can be measured either from thermal momentum distribution or from particle ratios [14]. Since expansion flow mimics some temperature [1], detailed analysis is needed to separate its effects. Here we concentrate on obtaining information from particle ratios

$$R_k^i \equiv \frac{N^i}{N^k} \quad (3.1)$$

as promised in the Introduction.

4. THE MODEL

After rehadronization the matter is a relativistic, interacting multicomponent hadronic mixture. It is difficult to describe this continuum, partly technically, partly because of lack of information. However, an earlier paper showed [14] that as far as specific entropy is concerned, a noninteracting relativistic Boltzmann mixture is tolerable, with cca. 10% error. Here we choose this approximation. Inclusion of mean field type interactions would not alter the structure [14], [15].

Our system is a Boltzmann mixture of particle species

$$\pi, N, \bar{N}, \Delta, \bar{\Delta}, \Lambda, \bar{\Lambda}, \Sigma, \bar{\Sigma}, K, \bar{K}, d$$

in complete thermal and chemical equilibrium. Therefore there would be 2 independent chemical potentials in the system, μ_q and μ_s [16], and the chemical potentials

of specific particle species are expressed as e.g.

$$\begin{aligned}\mu_N &= 3\mu_q \\ \mu_A &= 2\mu_q + \mu_s \\ \text{etc.} &\end{aligned}\tag{4.1}$$

The local state of such a matter can be described by 3 thermodynamic quantities (e.g. by the entropic intensives $\frac{1}{T}, \frac{-\mu_q}{T}, \frac{-\mu_s}{T}$). However, the initial state had 0 strangeness, therefore the final state will have too. So from practical viewpoint the number of independent variables is 2. Now we perform the transformation to the independent ratios.

Let us start with the independent coordinates

$$x^i = x^i (1/T, -\mu_q/T, -\mu_s/T) \tag{4.2}$$

Any specific density can be written as function of x^i ; then perform the transformation to x^i'

$$x^{i'} = x^{i'} \left(n' \equiv n^{\bar{K}} - n^K + n^A - n^{\bar{A}} + n^{\Sigma} - n^{\bar{\Sigma}}, R_{\pi^+}^{K^-}, R_K^{K^+} \right) \tag{4.3}$$

Our system is always at $x^{i'} = n^s \equiv 0$, and the further two coordinates of the state are just two particle ratios. The transformation $x^{i'} = x^{i'}(x^k)$ is regular if the matrix

$$\partial x^{i'}/\partial x^k$$

is regular. For our Boltzmann gas mixture and for the coordinate systems (4.2),(4.3) the regularity can be checked and holds.

Then we have introduced the observable ratios as coordinates in the thermodynamic state space; now our task is to express all other characteristics by them.

5. RESULTS

The main results of our calculations are displayed on the Figures. Fig. 1. displays the functional dependence among two mesonic ratios $R_{\pi^+}^{K^-}, R_K^{K^+}$ and temperature T. Henceforth we will always use these two mesonic ratios as independent variables for avoiding spectator particles in the ratios. Fig. 2. is the same but only for physically relevant temperatures up to 300 MeV. One can see that in a wide range to the same pair of particle ratios $(R_{\pi^+}^{K^-}, R_K^{K^+})$ two temperatures belong. This indicates that the thermodynamic state space in these variables covers at least two Riemannian

sheets. Observe that the ratio $R_{\pi^+}^{K^+}$ has a maximum value slightly dependent on $R_{K^+}^{K^-}$, cf. Fig. 3. According to our experience only 2 Riemannian sheets seem to exist, the manifold is displayed on Fig. 4.: the "low temperature" sheet is between the horizontal axis and the solid curve, the "high temperature" one is between the solid and dashed ones. The boundary between the two sheets is the state where $R_{\pi^+}^{K^+}$ is maximal. The temperature of these points vs. $R_{K^+}^{K^-}$ is shown on Fig. 5.; observe that at low $R_{K^+}^{K^-}$'s the second sheet starts at quite reasonable temperatures, so it cannot be *a priori* ignored. (However, the Tables of App. A show that these states are rather exotic for other parameters.) Fig. 6. shows the specific entropy $S/N(B)$ as function of the independent mesonic ratios for the low temperature sheet. (On the other sheet the range of specific entropy is roughly the same.) Finally, Fig. 7. is the same for the particle ratio $R_p^{K^+}$. This Figure clearly indicates that using $R_p^{K^+}$ instead of $R_{\pi^+}^{K^+}$ one would get at least two Riemannian sheets in place of the present low temperature one.

Of course, the Figures are only for bird's eye visual orientation; the numerical data, including a further particle ratio R_p^d , energy density ϵ , baryon density n and the two independent chemical potentials, μ_q, μ_s , can be found in Appendices A and B. It seems as if the stable d fragment would yield another experimental information; however this ratio needs some extra discussion, given in App. C.

Now, let us apply our method to the E802 experiment. There we have a value

$$R_{\pi^+}^{K^+} = 0.24 \pm 0.05$$

[17]. The second ratio can be evaluated from graphs showing the transverse momentum dependence of the ratios K^+/π^+ and K^-/π^- [18], assuming that positive and negative pions are equally abundant. Hence

$$R_{K^+}^{K^-} = 0.25 \pm 0.05$$

[19]. Finally, for the kaon/proton ratio one has a raw experimental date ~ 0.1 [17]. However, by a simple geometric model one expects as many spectator protons as participants [19], whence for local state one can estimate

$$R_p^{K^+} \sim 0.2$$

Now, the case $R_{K^+}^{K^-}=0.25$ can be found in details in App. B. (Cf. also Fig. 1.) Looking for the average second mesonic ratio, $R_{\pi^+}^{K^+} = 0.24$, one finds two possible states on the two sheets ($n_o = 0.145 \text{ fm}^{-3}$):

$$T = 118 \text{ MeV}, \quad S/N^B = 14, \quad n \sim 0.4n_o, \quad R_p^{K^+} = 0.21$$

$$T = 540 \text{ MeV}, \quad S/N^B = 7.5, \quad n \sim 426n_o, \quad R_p^{K^+} = 0.14$$

The first state is a quite reasonable breakup state, and the K^+ / p ratio is consistent with the other ratios. (Of course, it would be premature to conclude hence that complete thermodynamic equilibrium holds, but there is no evidence against it.) The second state is highly improbable for temperature, and, in the same time, the K^+ / p ratio is wrong. Therefore it seems probable that the particles were produced in the first state.

6. CONCLUSIONS

Here we have demonstrated that a detailed thermodynamic analysis of detected particle ratios can lead to the reconstruction of the local state from which the particles emerge. In our case, choosing proper variables, the result is almost unique. To apply this method we need two independent detected particle ratios for the reconstruction, and further ratios to check the equilibrium assumptions. Moreover, there is always the possibility that using ratios as thermodynamic variables the state space occupies more than one Riemannian sheets, and then the extra ratios can select the actual sheet. By this method one gets Tables, from which the familiar thermodynamic characteristics (entropy, temperature, &c.) can be found directly. Our specific Tables have been manufactured for a relativistic noninteracting Boltzmann mixture; a previous paper showed that this assumption causes moderate error ($\leq 10\%$) in the specific entropy. Futher investigations would be needed to estimate the errors in other parameters.

Applying the method on the available results to the E802 experiment, one obtains that the measured ratios are consistent with a breakup stage $T \approx (115-120)$ MeV, $n \sim 0.4n_o$, $S/N^B \sim 14$. Assuming isentropic expansion (quite satisfactory at lower beam energies), this specific entropy would be characteristic for the stage of maximal compression as well.

Up to now it is still open whether such an entropy can be produced in pure hadronic matter or the assumption of quark plasma is necessary.

APPENDIX A: Results of the Calculations — Tables

Let us consider a relativistic Boltzmann mixture of species $\alpha = 1 \dots \nu$, with degeneracy numbers d_α , particle rest masses m_α , chemical potentials μ_α in complete chemical equilibrium in the sense (4.1) and with a common temperature T , with vanishing strangeness. Then the sufficient number of local independent thermodynamical data is only 2, and we have chosen them as $R_{K^+}^{K^-}$ (upper left corner of Tables) and $R_{\pi^+}^{K^+}$ (first row). The further important quantities then can be calculated and tabulated below.

$$R_{K^+}^{K^-} = \frac{\frac{1}{2} \cdot n_K^-}{\frac{1}{2} \cdot n_K}$$

$$R_{\pi^+}^{K^+} = \frac{\frac{1}{2} \cdot n_K}{\frac{1}{2} \cdot (n_K + n_\Delta)}$$

$$R_{p^+}^{K^+} = \frac{\frac{1}{2} \cdot n_K}{\frac{1}{2} \cdot (n_K + n_\Delta)}$$

$$R_{d^+ p^+} = \frac{n_\Delta}{\frac{1}{2} \cdot (n_K + n_\Delta)}$$

$R_{K+}^{K-} = 0.05$

$R_{\pi+}^{K+}$	R_p^{K+}	R_p^d	S/N_B	$e \left[\frac{GeV}{fm^3} \right]$	$n \left[\frac{1}{fm^{-3}} \right]$	T	μ_q	μ_s
0.094	0.028	0.105	8.5	0.025	0.021	70.0	229.1	124.2
0.141	0.039	0.162	7.7	0.058	0.048	80.0	230.5	110.6
0.180	0.050	0.222	7.1	0.120	0.097	90.0	231.9	97.1
0.208	0.060	0.280	6.6	0.225	0.177	100.0	233.3	83.6
0.226	0.069	0.335	6.3	0.390	0.301	110.0	234.9	70.1
0.237	0.076	0.385	5.9	0.637	0.483	120.0	236.4	56.7
0.243	0.082	0.430	5.7	0.986	0.735	130.0	238.1	43.4
0.246	0.088	0.470	5.4	1.464	1.074	140.0	239.8	30.1
0.248	0.092	0.506	5.2	2.097	1.516	150.0	241.6	16.9
0.248	0.095	0.537	5.0	2.914	2.076	160.0	243.5	3.8
0.247	0.098	0.566	4.9	3.946	2.773	170.0	245.5	-9.2
0.246	0.101	0.592	4.7	5.227	3.624	180.0	247.6	-22.0
0.245	0.102	0.616	4.6	6.793	4.648	190.0	249.8	-34.8
0.243	0.104	0.638	4.4	8.62	5.866	200.0	252.1	-47.5
0.241	0.105	0.659	4.3	10.938	7.298	210.0	254.5	-60.0
0.239	0.106	0.679	4.2	13.606	8.969	220.0	257.1	-72.4
0.236	0.106	0.698	4.1	16.738	10.901	230.0	259.8	-84.7
0.234	0.107	0.717	4.0	20.386	13.122	240.0	262.6	-96.9

$R_{K+}^{K-} = 0.10$

$R_{\pi+}^{K+}$	R_p^{K+}	R_p^d	S/N_B	$e \left[\frac{GeV}{fm^3} \right]$	$n \left[\frac{1}{fm^{-3}} \right]$	T	μ_q	μ_s
0.073	0.042	0.050	11.7	0.013	0.009	70.0	211.6	131.0
0.119	0.059	0.077	10.4	0.029	0.021	80.0	210.5	118.4
0.165	0.075	0.105	9.6	0.058	0.042	90.0	209.5	105.8
0.205	0.090	0.133	9.0	0.106	0.075	100.0	208.4	93.3
0.238	0.103	0.159	8.6	0.141	0.125	110.0	207.5	80.3
0.262	0.114	0.183	8.2	0.291	0.197	120.0	206.5	68.4
0.280	0.123	0.204	7.9	0.446	0.297	130.0	205.7	56.0
0.293	0.131	0.223	7.6	0.658	0.429	140.0	205.0	43.8
0.302	0.137	0.240	7.3	0.936	0.600	150.0	204.3	31.6
0.308	0.142	0.255	7.1	1.296	0.816	160.0	203.8	19.6
0.312	0.146	0.269	6.9	1.749	1.084	170.0	203.4	7.7
0.314	0.149	0.282	6.7	2.314	1.411	180.0	203.1	-4.1
0.315	0.151	0.294	6.6	3.006	1.804	190.0	203.0	-15.7
0.315	0.153	0.306	6.4	3.846	2.273	200.0	203.1	-27.2
0.314	0.154	0.318	6.3	4.855	2.827	210.0	203.4	-38.4
0.312	0.155	0.329	6.2	6.058	3.475	220.0	203.8	-49.4
0.310	0.155	0.340	6.0	7.482	4.230	230.0	204.5	-60.3
0.307	0.154	0.351	5.9	9.156	5.104	240.0	205.4	-70.9

$R_{K+}^{K^-} = 0.15$

$R_{\pi+}^{K^+}$	$R_p^{K^+}$	R_p^d	S/N_B	$e \left[\frac{GeV}{fm^3} \right]$	$n \left[\frac{1}{fm^3} \right]$	T	μ_q	μ_s
0.062	0.054	0.031	14.7	0.009	0.006	70.0	200.9	134.4
0.104	0.076	0.048	12.9	0.019	0.013	80.0	198.2	122.3
0.150	0.097	0.066	11.8	0.039	0.025	90.0	195.6	110.2
0.193	0.116	0.084	11.1	0.070	0.045	100.0	193.0	98.2
0.232	0.133	0.100	10.5	0.119	0.075	110.0	190.5	86.2
0.263	0.147	0.115	10.0	0.191	0.118	120.0	188.1	74.2
0.289	0.159	0.128	9.6	0.291	0.177	130.0	185.7	62.4
0.309	0.169	0.140	9.3	0.428	0.255	140.0	183.4	50.6
0.324	0.177	0.151	9.0	0.608	0.355	150.0	181.3	39.0
0.336	0.183	0.161	8.7	0.840	0.482	160.0	179.3	27.5
0.344	0.188	0.170	8.5	1.134	0.639	170.0	177.5	16.2
0.350	0.192	0.179	8.3	1.502	0.831	180.0	175.8	5.1
0.354	0.194	0.187	8.1	1.955	1.063	190.0	174.4	-5.8
0.356	0.196	0.196	8.0	2.509	1.340	200.0	173.2	-16.5
0.356	0.196	0.204	7.8	3.179	1.669	210.0	172.3	-26.9
0.355	0.196	0.212	7.7	3.985	2.058	220.0	171.7	-37.0
0.353	0.195	0.220	7.5	4.947	2.512	230.0	171.4	-46.8
0.350	0.193	0.229	7.4	6.088	3.041	240.0	171.3	-56.4

$R_{K+}^{K^-} = 0.20$

$R_{\pi+}^{K^+}$	$R_p^{K^+}$	R_p^d	S/N_B	$e \left[\frac{GeV}{fm^3} \right]$	$n \left[\frac{1}{fm^3} \right]$	T	μ_q	μ_s
0.055	0.066	0.022	17.8	0.007	0.004	70.0	192.7	136.4
0.093	0.093	0.034	15.5	0.015	0.009	80.0	188.9	124.5
0.137	0.119	0.047	14.1	0.029	0.018	90.0	185.1	112.7
0.181	0.143	0.059	13.1	0.053	0.031	100.0	181.4	100.9
0.222	0.163	0.071	12.4	0.090	0.052	110.0	177.7	89.2
0.258	0.181	0.081	11.8	0.143	0.081	120.0	174.1	77.6
0.288	0.195	0.091	11.3	0.218	0.122	130.0	170.6	66.0
0.313	0.207	0.099	10.9	0.319	0.175	140.0	167.2	54.6
0.334	0.217	0.107	10.5	0.453	0.243	150.0	164.0	43.3
0.350	0.224	0.114	10.2	0.626	0.330	160.0	160.9	32.2
0.362	0.230	0.121	10.0	0.847	0.438	170.0	158.1	21.3
0.371	0.233	0.128	9.8	1.123	0.570	180.0	155.5	10.6
0.377	0.235	0.134	9.5	1.466	0.730	190.0	153.2	0.3
0.381	0.236	0.141	9.4	1.889	0.922	200.0	151.2	-9.8
0.383	0.235	0.147	9.2	2.405	1.151	210.0	149.5	-19.5
0.383	0.234	0.154	9.0	3.030	1.423	220.0	148.2	-28.8
0.381	0.231	0.161	8.9	3.783	1.743	230.0	147.3	-37.8
0.377	0.228	0.168	8.8	4.682	2.117	240.0	146.6	-46.5

$R_{K^+}^{K^-} = 0.25$

$R_{\pi^+}^{K^+}$	$R_p^{K^+}$	R_p^d	S/N_B	$e \left[\frac{GeV}{fm^3} \right]$	$n \left[\frac{1}{fm^3} \right]$	T	μ_q	μ_s
0.049	0.079	0.017	21.3	0.006	0.003	70.0	186.0	137.5
0.085	0.111	0.026	18.3	0.012	0.007	80.0	181.2	125.8
0.127	0.142	0.035	16.5	0.024	0.013	90.0	176.5	114.1
0.170	0.170	0.044	15.2	0.043	0.023	100.0	171.8	102.5
0.212	0.195	0.053	14.3	0.072	0.039	110.0	167.2	90.9
0.250	0.216	0.061	13.6	0.115	0.060	120.0	162.6	79.5
0.284	0.233	0.068	13.0	0.174	0.090	130.0	158.2	68.1
0.312	0.247	0.075	12.5	0.256	0.129	140.0	153.9	56.8
0.336	0.258	0.081	12.1	0.363	0.180	150.0	149.8	45.8
0.356	0.266	0.086	11.8	0.502	0.244	160.0	145.8	34.9
0.371	0.272	0.091	11.5	0.680	0.324	170.0	142.2	24.4
0.383	0.275	0.097	11.2	0.904	0.422	180.0	138.9	14.1
0.392	0.276	0.102	11.0	1.185	0.541	190.0	136.0	4.3
0.397	0.276	0.108	10.8	1.533	0.686	200.0	133.4	-5.2
0.400	0.273	0.113	10.6	1.962	0.859	210.0	131.3	-14.3
0.400	0.270	0.119	10.5	2.485	1.065	220.0	129.5	-23.0
0.399	0.265	0.125	10.3	3.121	1.308	230.0	128.2	-31.2
0.396	0.260	0.132	10.2	3.885	1.595	240.0	127.2	-39.1

$R_{K^+}^{K^-} = 0.30$

$R_{\pi^+}^{K^+}$	$R_p^{K^+}$	R_p^d	S/N_B	$e \left[\frac{GeV}{fm^3} \right]$	$n \left[\frac{1}{fm^3} \right]$	T	μ_q	μ_s
0.045	0.093	0.013	25.1	0.005	0.002	70.0	180.1	138.0
0.079	0.131	0.020	21.4	0.010	0.005	80.0	174.5	126.4
0.119	0.167	0.027	19.1	0.020	0.010	90.0	169.0	114.8
0.161	0.200	0.034	17.5	0.036	0.018	100.0	163.4	103.2
0.203	0.229	0.041	16.4	0.061	0.030	110.0	158.0	91.8
0.242	0.253	0.047	15.5	0.096	0.047	120.0	152.6	80.4
0.278	0.273	0.053	14.8	0.146	0.069	130.0	147.3	69.1
0.309	0.289	0.058	14.2	0.214	0.100	140.0	142.3	58.0
0.335	0.301	0.063	13.8	0.303	0.139	150.0	137.4	47.1
0.358	0.310	0.067	13.4	0.420	0.188	160.0	132.8	36.5
0.376	0.316	0.072	13.0	0.571	0.250	170.0	128.5	26.2
0.390	0.318	0.076	12.7	0.762	0.327	180.0	124.7	16.3
0.400	0.318	0.081	12.5	1.002	0.420	190.0	121.2	6.9
0.407	0.316	0.086	12.3	1.303	0.534	200.0	118.3	-2.1
0.411	0.311	0.091	12.1	1.677	0.670	210.0	115.8	-10.6
0.412	0.305	0.096	11.9	2.137	0.834	220.0	113.8	-18.6
0.411	0.298	0.102	11.8	2.698	1.028	230.0	112.3	-26.2
0.408	0.290	0.108	11.7	3.377	1.257	240.0	111.1	-33.3

$R_{K^+}^{K^-} = 0.35$

$R_{\pi^+}^{K^+}$	$R_p^{K^+}$	R_p^d	S/N_B	$e \left[\frac{GeV}{fm^3} \right]$	$n \left[\frac{1}{fm^3} \right]$	T	μ_q	μ_s
0.042	0.108	0.010	29.4	0.004	0.002	70.0	174.8	138.1
0.074	0.152	0.016	24.8	0.009	0.004	80.0	168.5	126.5
0.112	0.194	0.022	22.0	0.018	0.008	90.0	162.1	114.9
0.153	0.232	0.027	20.1	0.031	0.014	100.0	155.8	103.3
0.195	0.266	0.033	18.7	0.052	0.024	110.0	149.6	91.9
0.234	0.294	0.038	17.6	0.083	0.037	120.0	143.5	80.5
0.271	0.317	0.042	16.8	0.126	0.055	130.0	137.5	69.3
0.304	0.335	0.046	16.1	0.184	0.079	140.0	131.7	58.2
0.332	0.349	0.050	15.5	0.261	0.110	150.0	126.2	47.5
0.357	0.358	0.054	15.1	0.363	0.149	160.0	121.0	37.0
0.377	0.363	0.058	14.7	0.494	0.199	170.0	116.3	27.0
0.393	0.364	0.062	14.4	0.662	0.260	180.0	112.0	17.5
0.405	0.362	0.066	14.1	0.875	0.336	190.0	108.2	8.5
0.413	0.356	0.070	13.9	1.144	0.427	200.0	105.1	0.1
0.417	0.349	0.075	13.7	1.480	0.539	210.0	102.4	-7.8
0.419	0.340	0.080	13.6	1.897	0.672	220.0	100.3	-15.2
0.418	0.329	0.085	13.4	2.408	0.831	230.0	98.6	-22.1
0.416	0.319	0.091	13.3	3.029	1.019	240.0	97.4	-28.6

$R_{K^+}^{K^-} = 0.40$

$R_{\pi^+}^{K^+}$	$R_p^{K^+}$	R_p^d	S/N_B	$e \left[\frac{GeV}{fm^3} \right]$	$n \left[\frac{1}{fm^3} \right]$	T	μ_q	μ_s
0.040	0.125	0.008	34.4	0.004	0.002	70.0	169.8	137.8
0.070	0.176	0.013	28.7	0.008	0.003	80.0	162.8	126.1
0.106	0.225	0.017	25.3	0.016	0.007	90.0	155.7	114.5
0.146	0.269	0.022	22.9	0.028	0.012	100.0	148.7	102.9
0.187	0.308	0.026	21.3	0.046	0.019	110.0	141.8	91.4
0.227	0.340	0.031	20.0	0.073	0.030	120.0	135.0	80.0
0.264	0.367	0.034	19.0	0.111	0.044	130.0	128.3	66.8
0.298	0.387	0.038	18.2	0.162	0.064	140.0	121.9	57.8
0.328	0.402	0.041	17.6	0.230	0.089	150.0	115.8	47.1
0.354	0.411	0.044	17.0	0.320	0.121	160.0	110.2	36.9
0.376	0.414	0.047	16.6	0.437	0.161	170.0	105.0	27.1
0.393	0.413	0.051	16.3	0.588	0.211	180.0	100.4	18.0
0.406	0.407	0.055	16.0	0.782	0.273	190.0	96.5	9.4
0.416	0.398	0.059	15.8	1.028	0.349	200.0	93.2	1.5
0.421	0.387	0.063	15.6	1.338	0.441	210.0	90.4	-5.8
0.423	0.374	0.068	15.4	1.724	0.552	220.0	88.3	-12.5
0.423	0.360	0.073	15.3	2.200	0.684	230.0	86.6	-18.8
0.420	0.346	0.078	15.1	2.781	0.841	240.0	85.3	-24.6

$R_{K^+}^{K^-} = 0.50$

$R_{\pi^+}^{K^+}$	$R_p^{K^+}$	R_p^d	S/N_B	$e \left[\frac{GeV}{fm^3} \right]$	$n \left[\frac{1}{fm^3} \right]$	T	μ_q	μ_s
0.036	0.168	0.006	47.1	0.003	0.001	70.0	160.4	136.1
0.063	0.236	0.009	38.7	0.007	0.002	80.0	152.0	124.2
0.097	0.302	0.012	33.6	0.013	0.004	90.0	143.6	112.4
0.135	0.361	0.015	30.2	0.023	0.008	100.0	135.2	100.6
0.174	0.413	0.018	27.7	0.038	0.013	110.0	127.0	86.8
0.213	0.455	0.020	25.9	0.059	0.020	120.0	118.9	77.3
0.251	0.489	0.023	24.5	0.089	0.030	130.0	111.0	65.9
0.286	0.514	0.025	23.4	0.131	0.042	140.0	103.5	55.0
0.318	0.529	0.028	22.5	0.187	0.059	150.0	96.5	44.5
0.346	0.535	0.030	21.9	0.261	0.081	160.0	90.1	34.7
0.370	0.532	0.033	21.4	0.360	0.109	170.0	84.5	25.6
0.390	0.522	0.036	21.0	0.489	0.143	180.0	79.7	17.3
0.404	0.506	0.039	20.7	0.658	0.186	190.0	75.6	9.8
0.415	0.487	0.043	20.4	0.875	0.229	200.0	72.4	3.0
0.422	0.465	0.047	20.2	1.151	0.304	210.0	69.7	-3.1
0.425	0.443	0.051	20.1	1.497	0.383	220.0	67.7	-8.6
0.426	0.421	0.056	19.9	1.928	0.477	230.0	66.1	-13.6
0.424	0.400	0.061	19.8	2.458	0.589	240.0	64.9	-18.2

$R_{K^+}^{K^-} = 0.60$

$R_{\pi^+}^{K^+}$	$R_p^{K^+}$	R_p^d	S/N_B	$e \left[\frac{GeV}{fm^3} \right]$	$n \left[\frac{1}{fm^3} \right]$	T	μ_q	μ_s
0.033	0.230	0.004	65.9	0.003	0.001	70.0	150.9	133.0
0.058	0.323	0.006	53.4	0.006	0.002	80.0	141.2	120.7
0.090	0.413	0.008	45.8	0.011	0.003	90.0	131.4	108.4
0.125	0.494	0.010	40.7	0.019	0.005	100.0	121.7	96.2
0.163	0.564	0.012	37.1	0.032	0.008	110.0	112.2	84.1
0.202	0.621	0.014	34.5	0.050	0.013	120.0	102.8	72.2
0.239	0.663	0.015	32.4	0.075	0.020	130.0	93.9	60.7
0.275	0.690	0.017	30.9	0.110	0.028	140.0	85.5	49.7
0.308	0.700	0.019	29.7	0.158	0.040	150.0	77.9	39.6
0.337	0.695	0.021	28.9	0.223	0.055	160.0	71.3	30.4
0.362	0.677	0.024	28.2	0.311	0.074	170.0	65.6	22.2
0.382	0.650	0.026	27.8	0.428	0.098	180.0	61.0	15.0
0.398	0.617	0.030	27.5	0.582	0.128	190.0	57.3	8.8
0.410	0.582	0.033	27.2	0.783	0.165	200.0	54.4	3.3
0.417	0.547	0.037	27.1	1.039	0.211	210.0	52.1	-1.5
0.422	0.512	0.041	26.9	1.364	0.267	220.0	50.3	-5.9
0.423	0.480	0.045	26.7	1.770	0.335	230.0	49.0	-9.7
0.422	0.451	0.049	26.5	2.269	0.415	240.0	48.0	-13.3

$R_{K^+}^{K^-} = 0.70$

$R_{\pi^+}^{K^+}$	$R_p^{K^+}$	R_p^d	S/N_B	$e \left[\frac{GeV}{fm^3} \right]$	$n \left[\frac{1}{fm^3} \right]$	T	μ_q	μ_s
0.030	0.331	0.002	96.8	0.003	0.000	70.0	140.6	128.1
0.054	0.465	0.004	77.6	0.005	0.001	80.0	129.4	115.1
0.084	0.594	0.005	65.8	0.010	0.002	90.0	118.1	102.1
0.118	0.711	0.006	58.0	0.017	0.003	100.0	107.0	89.2
0.154	0.809	0.008	52.4	0.028	0.005	110.0	96.1	76.5
0.191	0.885	0.009	48.3	0.043	0.009	120.0	85.6	64.2
0.228	0.934	0.010	45.3	0.065	0.013	130.0	75.7	52.5
0.264	0.953	0.012	43.1	0.096	0.018	140.0	66.8	41.8
0.297	0.943	0.013	41.5	0.139	0.026	150.0	59.2	32.4
0.326	0.909	0.015	40.4	0.199	0.039	160.0	52.9	24.3
0.352	0.859	0.017	39.6	0.280	0.049	170.0	47.8	17.5
0.373	0.801	0.020	39.1	0.390	0.065	180.0	43.9	11.8
0.389	0.741	0.023	38.7	0.536	0.086	190.0	40.8	6.9
0.402	0.684	0.026	38.5	0.727	0.111	200.0	38.5	2.8
0.410	0.630	0.029	38.3	0.973	0.143	210.0	36.7	-0.7
0.415	0.582	0.033	38.0	1.285	0.181	220.0	35.4	-3.9
0.417	0.538	0.037	37.8	1.675	0.227	230.0	34.4	-6.7
0.417	0.500	0.041	37.6	2.157	0.283	240.0	33.6	-9.2

$R_{K^+}^{K^-} = 0.80$

$R_{\pi^+}^{K^+}$	$R_p^{K^+}$	R_p^d	S/N_B	$e \left[\frac{GeV}{fm^3} \right]$	$n \left[\frac{1}{fm^3} \right]$	T	μ_q	μ_s
0.028	0.528	0.001	157.3	0.002	0.000	70.0	128.2	120.4
0.051	0.743	0.002	125.0	0.005	0.001	80.0	115.1	106.2
0.079	0.952	0.003	105.3	0.009	0.001	90.0	102.0	92.0
0.111	1.135	0.004	91.8	0.015	0.002	100.0	89.2	78.0
0.146	1.282	0.004	82.5	0.024	0.003	110.0	76.8	64.5
0.182	1.378	0.005	75.7	0.038	0.005	120.0	65.2	51.8
0.219	1.411	0.006	70.8	0.058	0.008	130.0	54.9	40.4
0.254	1.380	0.007	67.3	0.086	0.011	140.0	46.4	30.8
0.286	1.301	0.009	64.9	0.126	0.016	150.0	39.7	23.0
0.315	1.196	0.011	63.3	0.183	0.022	160.0	34.6	16.8
0.341	1.084	0.013	62.3	0.261	0.029	170.0	30.8	11.9
0.362	0.976	0.015	61.6	0.367	0.039	180.0	28.0	7.9
0.379	0.878	0.018	61.1	0.508	0.052	190.0	25.9	4.7
0.392	0.791	0.021	60.7	0.694	0.068	200.0	24.3	2.0
0.402	0.716	0.024	60.3	0.934	0.088	210.0	23.1	-0.3
0.407	0.651	0.028	59.9	1.239	0.112	220.0	22.2	-2.3
0.410	0.595	0.031	59.5	1.620	0.141	230.0	21.6	-4.1
0.410	0.547	0.035	59.0	2.092	0.176	240.0	21.1	-5.7

$R_{K+}^{K-} = 0.90$

$R_{\pi+}^{K+}$	R_p^{K+}	R_p^d	S/N_B	$\epsilon \left[\frac{GeV}{fm^3} \right]$	$n \left[\frac{1}{fm^3} \right]$	T	μ_q	μ_s
0.027	1.127	0.001	341.6	0.002	0.000	70.0	109.1	105.4
0.048	1.568	0.001	265.6	0.004	0.000	80.0	93.6	89.4
0.075	2.010	0.001	222.5	0.008	0.000	90.0	77.8	73.1
0.106	2.361	0.002	192.5	0.014	0.001	100.0	62.8	57.5
0.139	2.563	0.002	171.7	0.022	0.001	110.0	49.2	43.4
0.175	2.561	0.003	157.1	0.035	0.002	120.0	38.0	31.7
0.210	2.382	0.004	147.0	0.053	0.003	130.0	29.7	22.8
0.244	2.114	0.005	140.0	0.080	0.005	140.0	23.8	16.4
0.276	1.831	0.006	135.4	0.119	0.007	150.0	19.7	11.8
0.305	1.575	0.008	132.3	0.174	0.010	160.0	16.8	8.4
0.330	1.356	0.010	130.1	0.251	0.014	170.0	14.8	5.9
0.351	1.175	0.012	128.5	0.355	0.018	180.0	13.4	3.9
0.369	1.026	0.014	127.1	0.494	0.025	190.0	12.3	2.3
0.382	0.904	0.017	125.8	0.678	0.032	200.0	11.5	1.0
0.392	0.803	0.020	124.4	0.914	0.042	210.0	10.9	-0.1
0.399	0.720	0.024	122.8	1.215	0.054	220.0	10.5	-1.1
0.402	0.651	0.027	121.0	1.593	0.068	230.0	10.2	-1.9
0.403	0.592	0.030	119.1	2.059	0.086	240.0	10.0	-2.7

$R_{K+}^{K-} = 1.00$

$R_{\pi+}^{K+}$	R_p^{K+}	R_p^d	S/N_B	$\epsilon \left[\frac{GeV}{fm^3} \right]$	$n \left[\frac{1}{fm^3} \right]$	T	μ_q	μ_s
0.033	62.876	0.000	9999.9	0.002	0.000	70.0	0.0	0.0
0.046	45.385	0.000	9999.9	0.004	0.000	80.0	0.0	0.0
0.071	25.523	0.000	9999.9	0.007	0.000	90.0	0.0	0.0
0.101	14.745	0.000	9999.9	0.013	0.000	100.0	0.0	0.0
0.133	9.305	0.001	9999.9	0.021	0.000	110.0	0.0	0.0
0.167	6.285	0.001	9999.9	0.033	0.000	120.0	0.0	0.0
0.201	4.481	0.002	9999.9	0.052	0.000	130.0	0.0	0.0
0.234	3.337	0.003	9999.9	0.078	0.000	140.0	0.0	0.0
0.265	2.576	0.004	9999.9	0.117	0.000	150.0	0.0	0.0
0.294	2.048	0.006	9999.9	0.172	0.000	160.0	0.0	0.0
0.319	1.671	0.007	9999.9	0.248	0.000	170.0	0.0	0.0
0.340	1.392	0.010	6795.5	0.352	0.000	180.0	0.0	0.0
0.358	1.182	0.012	4748.5	0.490	0.001	190.0	0.0	0.0
0.372	1.019	0.015	3462.0	0.673	0.001	200.0	0.0	0.0
0.382	0.891	0.017	2626.4	0.908	0.002	210.0	0.0	0.0
0.389	0.788	0.020	2051.8	1.208	0.003	220.0	0.0	0.0
0.394	0.705	0.024	1646.2	1.584	0.005	230.0	0.0	0.0
0.395	0.637	0.027	1350.8	2.049	0.008	240.0	0.0	0.0

APPENDIX B: Table for $R_{K^+}^{K^-} = 0.25$

$R_{K^+}^{K^-} = 0.25$

$R_{\pi^+}^{K^+}$	$R_p^{K^+}$	R_p^t	S/N_B	$e \left[\frac{GeV}{fm^3} \right]$	$n \left[\frac{1}{fm^3} \right]$	T	μ_η	μ_s
0.023	0.049	0.009	26.7	0.002	0.001	60.0	190.7	149.1
0.085	0.111	0.026	18.3	0.012	0.007	80.0	181.2	125.8
0.170	0.170	0.044	15.2	0.043	0.023	100.0	171.8	102.5
0.250	0.216	0.061	13.6	0.115	0.060	120.0	162.6	79.5
0.312	0.247	0.075	12.5	0.256	0.129	140.0	153.9	56.8
0.356	0.266	0.086	11.8	0.502	0.244	160.0	145.8	34.9
0.383	0.275	0.097	11.2	0.904	0.422	180.0	138.9	14.1
0.397	0.276	0.108	10.8	1.533	0.686	200.0	133.4	-5.2
0.400	0.270	0.119	10.5	2.485	1.065	220.0	129.5	-23.0
0.396	0.260	0.132	10.2	3.885	1.595	240.0	127.2	-39.1
0.386	0.247	0.146	9.9	5.880	2.317	260.0	126.3	-53.9
0.373	0.234	0.160	9.7	8.642	3.276	280.0	126.6	-67.5
0.359	0.222	0.175	9.5	12.366	4.522	300.0	127.9	-80.1
0.344	0.210	0.190	9.2	17.265	6.105	320.0	129.8	-92.0
0.330	0.200	0.206	9.0	23.571	8.080	340.0	132.4	-103.3
0.317	0.190	0.221	8.8	31.535	10.501	360.0	135.4	-114.1
0.305	0.181	0.236	8.6	41.425	13.427	380.0	138.8	-124.6
0.294	0.174	0.251	8.5	53.527	16.913	400.0	142.5	-134.7
0.284	0.167	0.265	8.3	68.140	21.018	420.0	146.5	-144.6
0.274	0.161	0.279	8.1	85.584	25.801	440.0	150.6	-154.4
0.266	0.155	0.293	8.0	106.190	31.318	460.0	154.9	-163.9
0.258	0.150	0.306	7.8	130.307	37.629	480.0	159.4	-173.3
0.251	0.146	0.319	7.7	158.298	44.791	500.0	163.9	-182.6
0.245	0.142	0.331	7.5	190.544	52.861	520.0	168.6	-191.8
0.239	0.138	0.343	7.4	227.436	61.896	540.0	173.4	-200.9
0.234	0.135	0.354	7.3	269.384	71.954	560.0	178.2	-210.0
0.229	0.132	0.365	7.2	316.811	83.090	580.0	183.1	-218.9
0.224	0.130	0.376	7.1	370.155	95.359	600.0	188.0	-227.9
0.220	0.127	0.386	7.0	429.870	108.817	620.0	193.0	-236.7
0.216	0.125	0.396	6.9	496.423	123.518	640.0	198.1	-245.5
0.213	0.123	0.405	6.8	570.297	139.515	660.0	203.2	-254.3
0.210	0.121	0.414	6.7	651.988	156.864	680.0	208.3	-263.1
0.207	0.119	0.423	6.7	742.011	175.616	700.0	213.4	-271.8
0.204	0.118	0.431	6.6	840.889	195.825	720.0	218.6	-280.5
0.202	0.116	0.439	6.5	949.166	217.541	740.0	223.8	-289.1
0.199	0.115	0.446	6.4	999.999	240.818	760.0	229.0	-297.8
0.197	0.113	0.454	6.4	999.999	265.707	780.0	234.3	-306.4

Appendix C

THE DEUTERON/PROTON RATIO

The d/p ratio seems convenient to measure specific entropy [12], since both particles are stable. However, deuterons are not too appropriate for such measurement because of their large "volume" (meaning $\sigma_{break-up}^{3/2}$). Dimensional analysis considerations suggest that V_d may appear in the equation of state even if the deuteron component is actually dilute and that the error of ideal gas formulae for S/N from R_d^d is ~ 3 [20]. Correlation volume calculations [21] demonstrate that the deuteron "volume" should indeed appear in the equation of state, and a comparison of measurements and ideal gas calculations in fact shows the d suppression below 2 GeV/nucl beam energy [22].

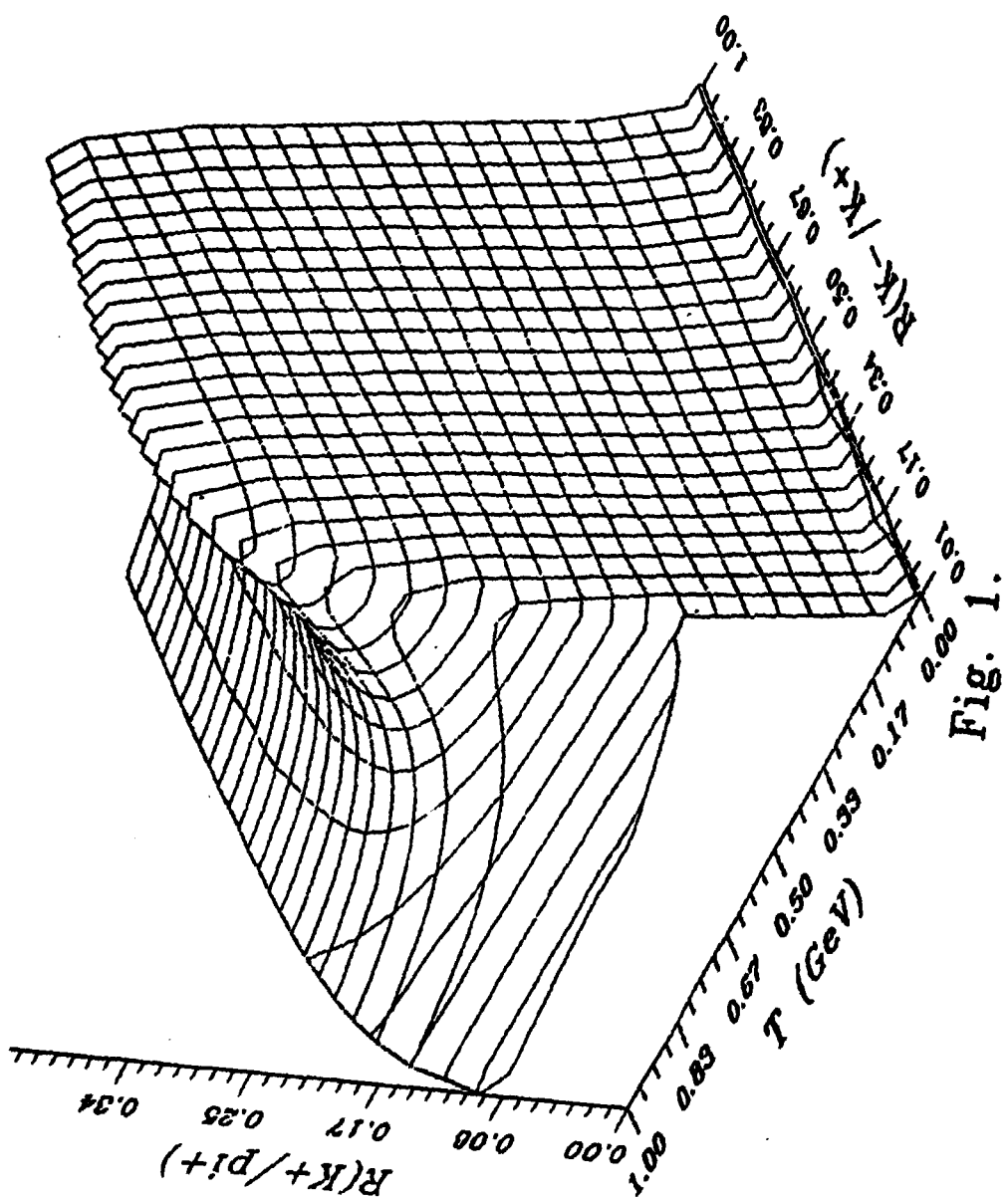
However, this suppression seems to vanish at 2.1 GeV/nucl bombarding energy. The reason behind this would deserve some study (may be it is the decrease of break-up cross section with increasing relative velocities i.e. temperature); however for our present goal we may be simply encouraged by the observed agreement to list R_d , obtained from a Boltzmann approximation.

REFERENCES

- [1] J.P.Bondorf, S.I.A.Garpman and J.Zimányi, Nucl.Phys. **A296**, 320 (1978)
- [2] T.Biró, H.W.Barz, B.Lukács and J.Zimányi, Phys.Rev. **C27**, 2695 (1983)
- [3] U. Heinz, K. S. Lee and E. Schnedermann, TPR-89-13
- [4] Yu. B. Ivanov, I. N. Mishustin and L. M. Satarov, Nucl. Phys. **A433**, 713 (1985)
- [5] J.B.Callen, Thermodynamics. Wiley, N.Y. 1960.
- [6] F.Weinhold, J.Chem.Phys. **63**, 2479 (1975)
- [7] L.Diósi, G.Forgács, B.Lukács and H.L.Frisch, Phys.Rev. **A29**, 3343 (1984)
- [8] L.Diósi and B.Lukács, Phys.Rev. **A31**, 3415 (1985)
- [9] B.Lukács and K.Martinás, Phys.Lett. **114A**, 306 (1986)
- [10] B.Lukács, K.Martinás, G.Paál, Relativity Today, ed. Z.Perjés, World Scientific, Singapore, 1988, p. 247.
- [11] L.P.Eisenhardt, Riemannian Geometry. Princeton University Press, 1950
- [12] P. J. Siemens and J. I. Kapusta, Phys. Rev. Lett. **43**, 1386 (1979)
- [13] L. P. Csernai, B. Lukács and J.Zimányi, Lett. Nuovo Cimento **27**, 11 (1980)
- [14] P.Lévai, B.Lukács, J.Zimányi and U.Heinz, KFKI-89-22 in press in Z.Phys. A.
- [15] J.Zimányi, B.Lukács, P.Lévai, J.P.Bondorf, N.L.Balázs
Nucl.Phys. **A484**, 647, (1988)
- [16] B.Lukács, J.Zimányi and N.L.Balázs, Phys.Lett. **B183**, 27 (1987)
- [17] M. J. Tannenbaum, BNL-41608-88
- [18] Y.Akiba et al. Annual Report, Inst. for Nuclear Study, Univ. of Tokyo, 1988 p.43.
- [19] P.Lévai, Lecture on 6th Nordic Meeting, Norway, 1989. to appear in Physica Scripta
- [20] B.Lukács, Proc. VI. Balaton Conf. 1983, ed. J. Erő, p.367
- [21] L.Diósi and B.Lukács, J.Chem.Phys. **84**, 5081 (1986)
- [22] H-W.Barz,T.S.Biró,B.Lukács and J.Zimányi, Acta Phys.Hung. **62**, 373 (1987)

Figure Captions

- Fig.1. : Functional dependence among the thermodynamic variables R_{K+}^{K-} , $R_{\pi+}^{K+}$ (mesonic ratios) and temperature T. Lines denote constant mesonic ratios. Observe that in a wide range of them there exist two temperatures belonging to the same ratios, indicating the existence of (at least) two Riemannian sheets on the manifold. A related phenomenon is that $R_{\pi+}^{K+}$ possesses a maximum inside the manifold.
- Fig.2. : As Fig. 2, but only the physically relevant part up to T=300 MeV.
- Fig.3. : Temperature vs. ratio $R_{\pi+}^{K+}$ at several fixed values of the ratio R_{K+}^{K-} . The specific values are: $R_{K+}^{K-} = 0.05$ — solid line; $R_{K+}^{K-} = 0.15$ — long dash; $R_{K+}^{K-} = 0.25$ — medium dash; $R_{K+}^{K-} = 0.35$ — short dash.
- Fig.4. : The positions of the two Riemannian sheets in the coordinate space of mesonic ratios. The "low temperature" sheet is between the horizontal axis and the solid line, the "high temperature" one is between the solid and dashed lines. The matching is on the solid line. The right boundary has not been calculated.
- Fig.5. : The temperature at the matching of the two sheets vs. R_{K+}^{K-} . Observe that, except for very small ratios, on the "high temperature" sheet T is always above 200 MeV, but not necessarily very far from it.
- Fig.6. : Specific entropy S/N(B) vs. mesonic ratios on the low temperature sheet. The range of entropy values is roughly similar on the other sheet too. For details see App. A.
- Fig.7. : Particle ratio R_p^{K+} vs. the mesonic ratios on the low temperature sheet. Details again in App. A. Observe that exchanging $R_{\pi+}^{K+}$ to R_p^{K+} even this sheet would be doubled.



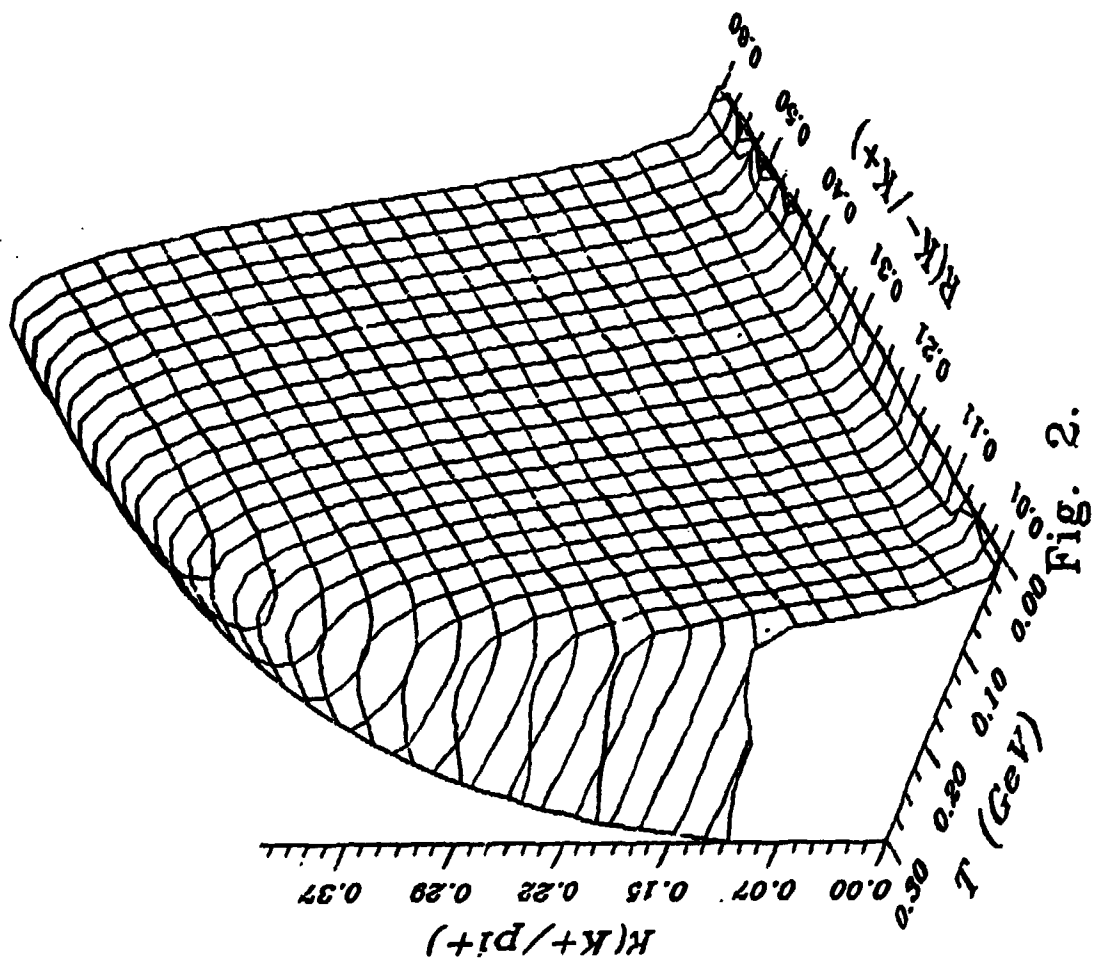


Fig. 2i

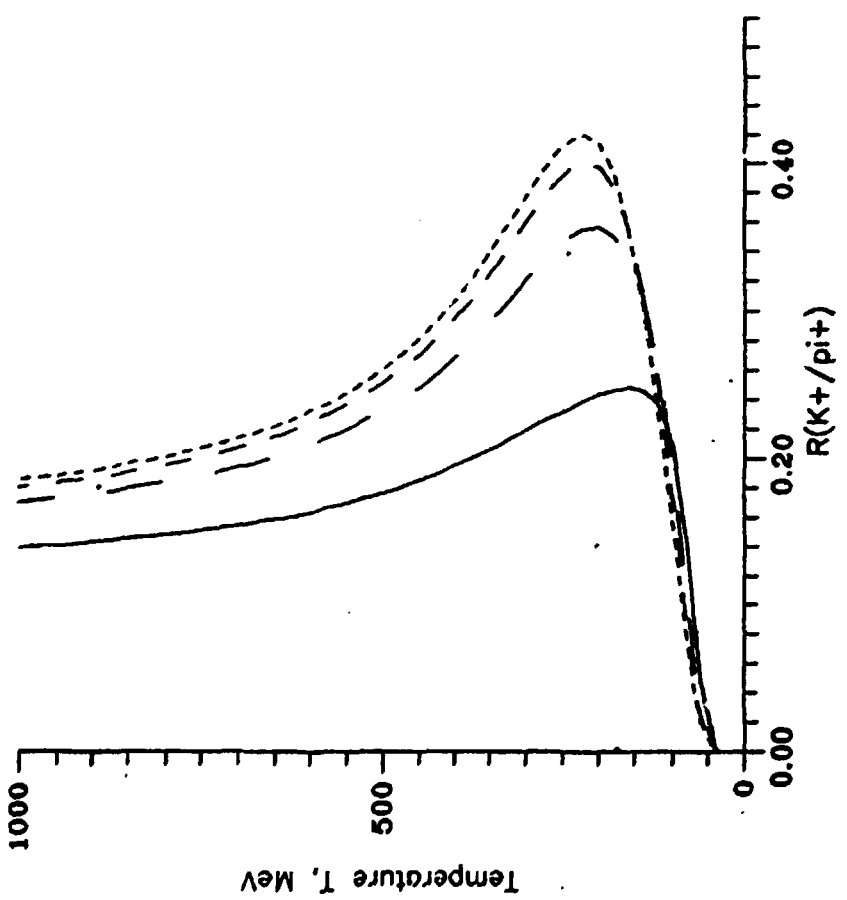


Fig. 3

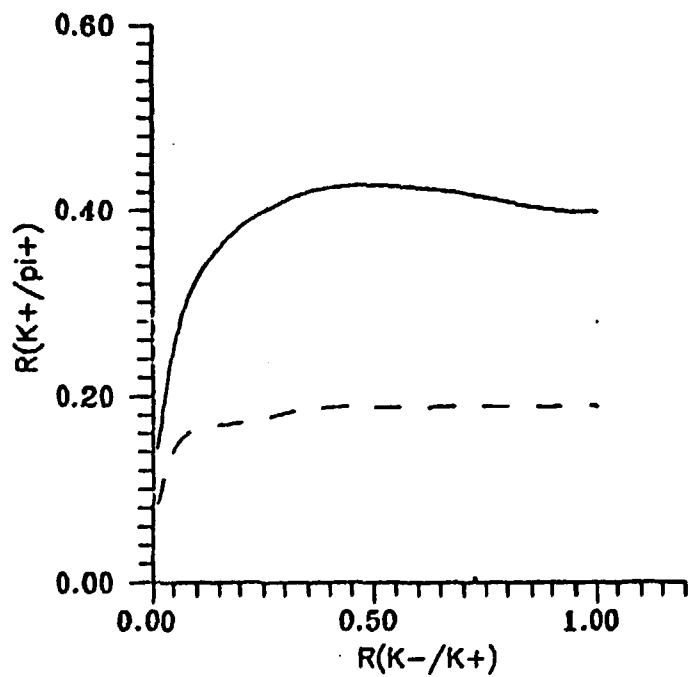


Fig. 4

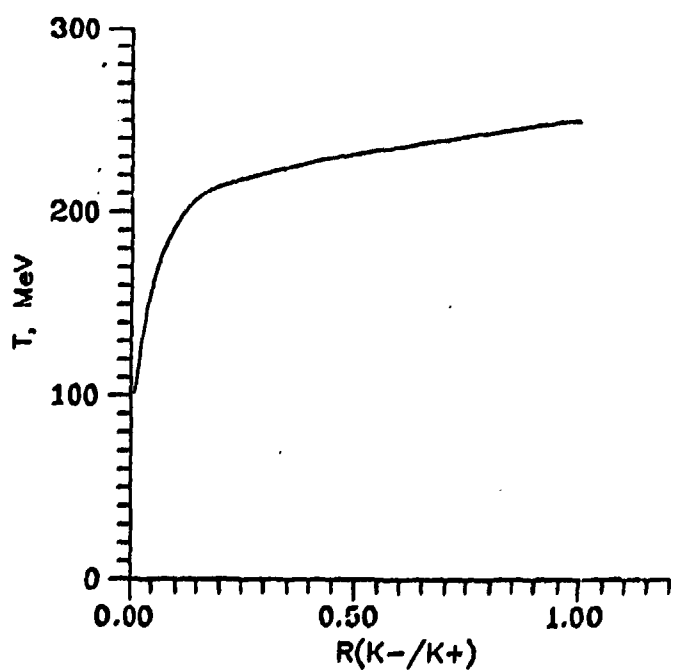
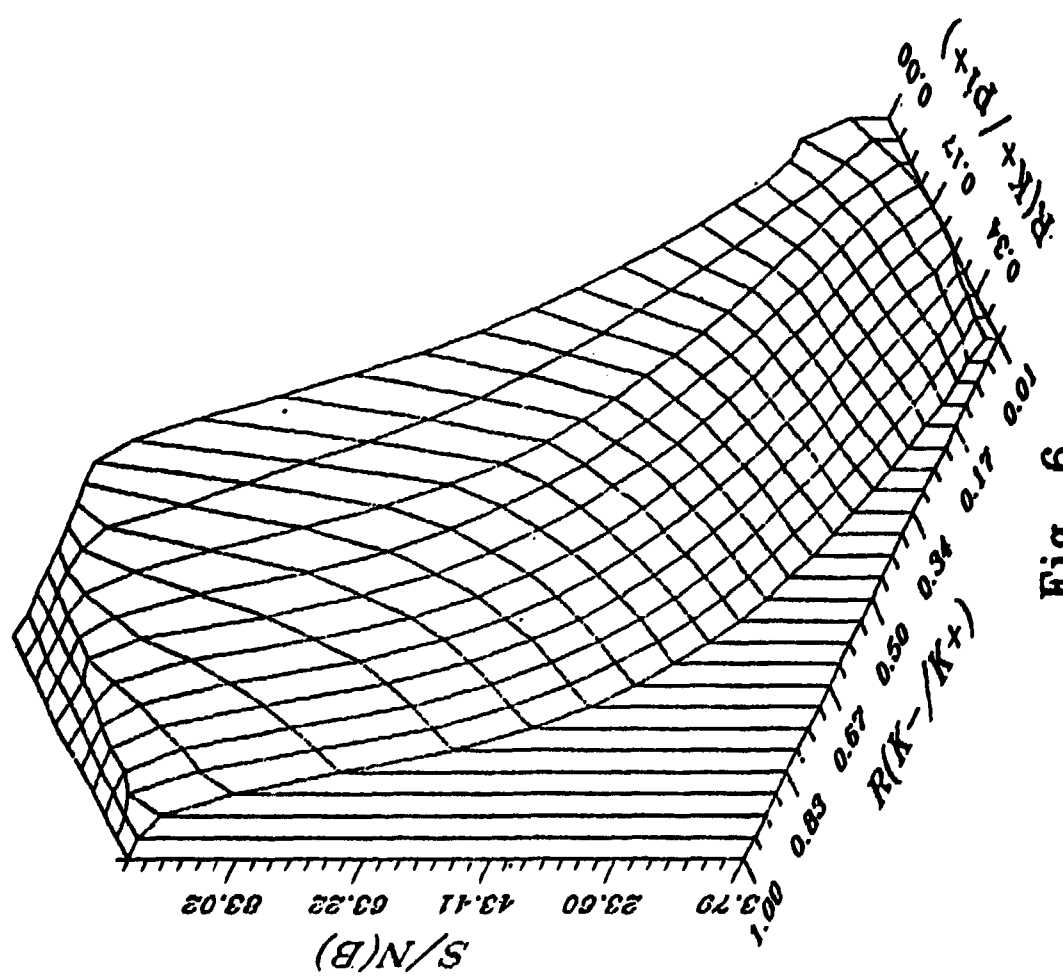


Fig. 5

Fig. 6.



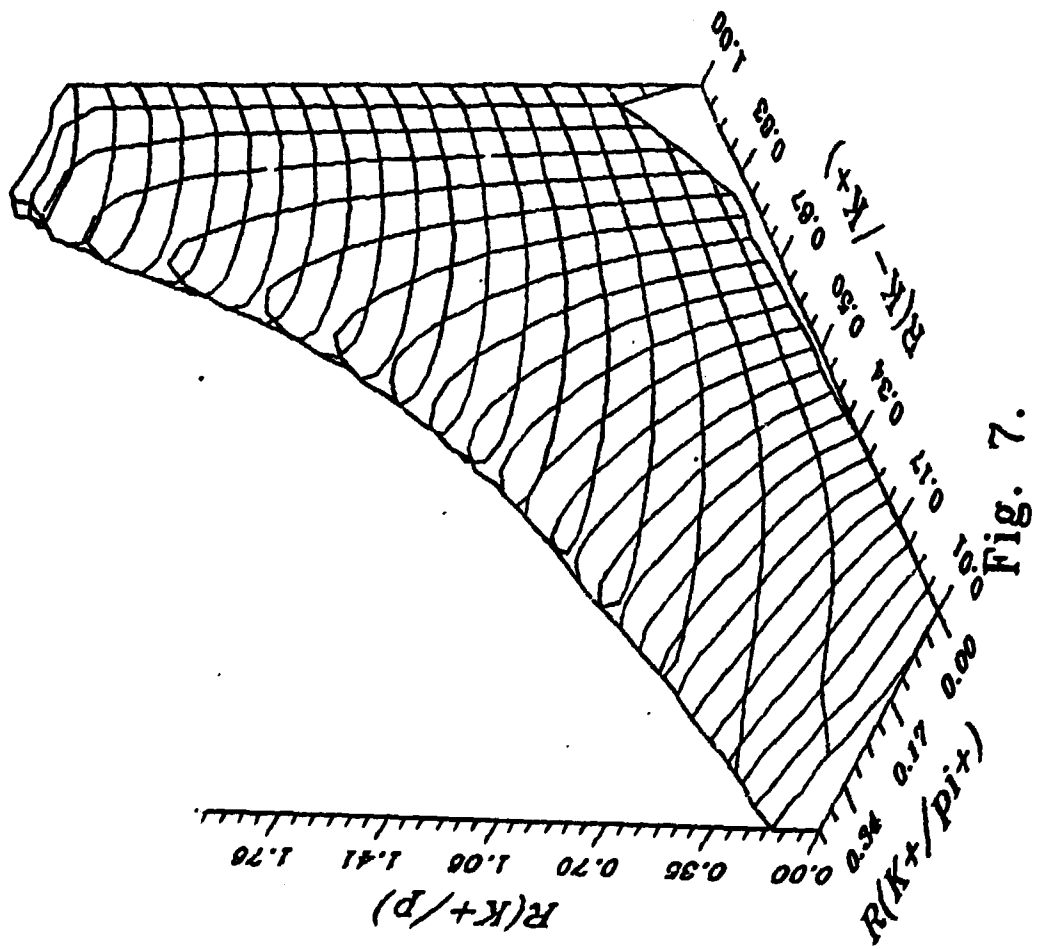


Fig. 7.

The issues of the KFKI preprint/report series are classified as follows:

- A. Particle and Nuclear Physics
- B. General Relativity and Gravitation
- C. Cosmic Rays and Space Research
- D. Fusion and Plasma Physics
- E. Solid State Physics
- F. Semiconductor and Bubble Memory Physics and Technology
- G. Nuclear Reactor Physics and Technology
- H. Laboratory, Biomedical and Nuclear Reactor Electronics
- I. Mechanical, Precision Mechanical and Nuclear Engineering
- J. Analytical and Physical Chemistry
- K. Health Physics
- L. Vibration Analysis, CAD, CAM
- M. Hardware and Software Development, Computer Applications, Programming
- N. Computer Design, CAMAC, Computer Controlled Measurements

The complete series or issues discussing one or more of the subjects can be ordered; institutions are kindly requested to contact the KFKI Library, individuals the authors.

Title and classification of the issues published this year:

- KFKI-1989-01/D G. Kocsis et al.: A possible method for ion temperature measurement by ion sensitive probes
- KFKI-1989-02/G L. Perneczky et al.: Using the pressurizer spray line in order to minimize loop-seal effects (in Hungarian)
- KFKI-1989-03/E T. Csiba et al.: Propagation of charge-density wave voltage noise along a blue bronze, $Rb_0.3MoO_3$ crystal
- KFKI-1989-04/G G. Baranyai et al.: Experimental investigation of leakage of safety valves by means of acoustic emission detectors (in Hungarian)
- KFKI-1989-05/A Nguyen Ai Viet et al.: Can solutions exist in non linear models constructed by the non-linear invariance principle?
- KFKI-1989-06/A Nguyen Ai Viet et al.: A non-linearly invariant Skyrme type model
- KFKI-1989-07/A Nguyen Ai Viet et al.: Static properties of nucleons in a modified Skyrme model
- KFKI-1989-08/B Z. Perjés: Factor structure of the Tomimatsu-Sato metrics
- KFKI-1989-09/B Z. Perjés: Unitary spinor methods in general relativity
- KFKI-1989-10/G G. Baranyai et al.: Reflooding investigations. Part I. (in Hungarian)
- KFKI-1989-11/G L. Maróti et al.: Description of the physical models applied in the COCONT code. (in Hungarian)

KFKI-1989-13/G L. Maróll et al.: Operational procedure based on hot spot analysis at the WWER-440 type block of Paks Nuclear Power Plant. Part III. (In Hungarian)

KFKI-1989-14/A Cs. Balázs: Lessons from a time dependent model

KFKI-1989-15/A V.Sh. Goyokhia: Quark confinement and dynamical breakdown of chiral symmetry in covariant gauge QCD

KFKI-1989-16/A A. Frenkel: Spontaneous localizations of the wave function and classical behavior

KFKI-1989-17/D S. Kálvin et al.: USX and SX radiation measurement of tokamak plasma by MicroChannel Plate

KFKI-1989-18/A S.I. Bastrukov et al.: Liquid layer model for non magic nuclei

KFKI-1989-19/G E. Biró et al.: Summary of VVER 1000 data compiled by CRIP on the basis of international cooperation. (In Hungarian)

KFKI-1989-20/M M. Barbuceanu et al.: Concurrent refinement of structured objects: a declarative language for knowledge systems programming

KFKI-1989-21/C K.I. Gringauz et al.: The analysis of the neutral gas measurements near comet P/Halley based on observations by VEGA-1

KFKI-1989-22/A P. Léval et al.: A simple expression for the entropy of a fireball from experimental strange particle ratios

KFKI-1989-23/M L.Zs. Varga et al.: Knowledge based techniques in network management

KFKI-1989-24/A J. Réval: Exactly soluble model of a quantum system in external field with periodic time dependence

KFKI-1989-25/J Sz. Vass, T. Török, Gy. Jákli, E. Berecz: Sodium alkylsulphate apparent molar volumes in normal and heavy water. Connection with micellar structure

KFKI-1989-26/A Gy. Kluge: On prompt fission neutrons

KFKI-1989-27/A S. Krasznovszky, I. Wagner: Description of the scaled moments for the nondiffractive $p\bar{p}$ and $\bar{p}p$ interactions in the cms energy range 10-800 GeV

KFKI-1989-28/E D.V. Shchoput et al.: Acousto-optical properties of Ge-As-S glasses and some possible applications

KFKI-1989-29/C B. Lukács: A note on ancient Egyptians' colour vision

KFKI-1989-30/G L. Szabados et al.: 7.4% hot leg break without SITs in action. (In Hungarian)

KFKI-1989-31/G L. Szabados et al.: 7.4% hot leg break with SITs in action. (In Hungarian)

KFKI-1989-32/A V.V. Anisovich: Quark model and QCD

KFKI-1989-33/G L. Szabados et al.: Comparison of experimental results on the PMK NVH stand in case of 7.4% hot and cold leg breaks. (In Hungarian)

- KFKI-1989-34/A** T. Csörgő et al.: Fragmentation of target spectators in ultrarelativistic heavy ion collisions
- KFKI-1989-35/C** E. Merényi et al.: The landscape of comet Halley
- KFKI-1989-36/C** K. Szegő: P/Halley the model comet, In view of the imaging experiment aboard the VEGA spacecraft
- KFKI-1989-37/K** S. Deme et al.: Reliability of real-time computing with radiation data feedback at accidental release
- KFKI-1989-38/G,I** P. Pellionisz et al.: Interpretation of acoustic emission signals to the evaluation of pressure tests. (In Hungarian)
- KFKI-1989-39/G** A. Péter: Experiments on acoustic emission detectors. (In Hungarian)
- KFKI-1989-40/A** S.I. Bastrukov et al.: Fluid-dynamics of the nuclear surface Fermi-layer
- KFKI-1989-41/D** D. Hildebrandt et al.: Impurity flux collection at the plasma edge of the tokamak MT-1
- KFKI-1989-42/I** L. Cser et al.: Monte Carlo modelling for neutron guide losses
- KFKI-1989-43/G** L. Perneczky et al.: SB LOCA analyses for Paks NPP. 7.4% hot leg break without SITs in action. (In Hungarian)
- KFKI-1989-44/G** L. Szabados et al.: 3.5% cold leg brak without SITs in action. (In Hungarian)
- KFKI-1989-45/A** V.Sh. Gogokhia: Gauge invariant, nonperturbative approach to the infrared-finite bound state problem in QCD
- KFKI-1989-46/G** S. Lipcsei et al.: Studies on vibration of fuel rods. I. Mechanical models of vibration of fuel rods in PWRs. (in Hungarian)
- KFKI-1989-47/A** P. Léval et al.: Entropy content from strange particle ratios in the E802 experiment

Kiadja a Központi Fizikai Kutató Intézet
Felelős kiadó: Szegő Károly
Szakmai lektor: Lovas István
Nyelvi lektor: Csörgő Tamás
Példányszám: 333 Törzsszám: 89-353
Készült a KFKI sokszorosító üzemében
Feltölts vezető: Gonda Péter
Budapest, 1989. szeptember hó